2005 American Control Conference
June 8-10, 2005. Portland, OR, USA

Current versus Flux in the Control of Electromechanical Valve Actuators

Katherine S. Peterson, Anna G. Stefanopoulou, Jim Freudenberg

Abstract— **Due to a lack of bandwidth separation, it is unclear which combination of feedback signals would be most advantageous for controlling electromechanical valve actuators. To address this issue, this paper investigates the use of position, current, and flux measurements in the feedback. Based on the analysis, a combination of position and flux best achieves the design specifications without incurring large control signals.**

I. Introduction

The electromagnetic valve actuator (EVA), shown in Fig. 1, has recently received attention due to its ability to significantly improve the performance of a standard internal combustion (IC) engine [5], [15]. Valve timing in most automotive engines is controlled via the camshaft, which couples the valve timing to the motion of the crankshaft. Although this ensures that the valves open and close at the correct time, the fixed valve timing results in a performance trade-off between idle and high speed operation. Through the use of electromagnets, the EVA de-couples the valve timing from the crankshaft for greater flexibility and improved performance [5], [15].

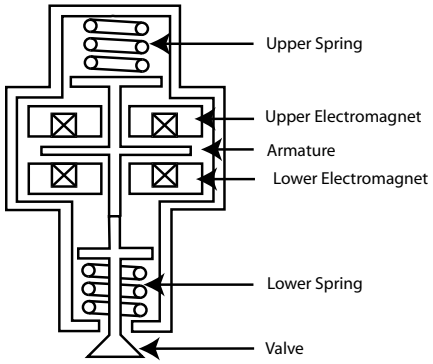

Fig. 1. Electromagnetic Valve Actuator.

The EVA consists of an armature mounted between two sets of springs and electromagnets. The preload on each spring is set such that the armature sits at rest equidistant from either electromagnet. In the valve closed position, the armature is held against the upper coil causing the upper spring to be more compressed than the lower spring. To open the valve, voltage to the upper coil is turned off and the armature is driven toward the lower coil by the force imbalance in the springs. A voltage is then applied to the lower coil to catch the armature and hold the valve in the open position. The process is then reversed to close the valve [15].

Near the electromagnet the system is unstable [13]. If not properly controlled, the instability causes the armature to accelerate in an unbounded fashion toward the electromagnet, resulting in impacts of up to 1-2 m/s [15]. Besides potentially damaging the actuator, these impacts are unacceptably loud [15]. Numerous controllers have been proposed to eliminate these impacts, such as sensor-less [2], [7], LQR [11], [13], nonlinear [9], self-adjusting [4], [10], and H_∞ [6]. This paper examines the use of various feedback signals for controlling the EVA. Specifically we consider combinations of position, current, and magnetic flux in the feedback.

The paper is organized as follows; Both a current based and magnetic flux based model of the EVA are presented in Sec. II. Based on the design specifications given in Sec. III, it is shown that a combination of either position and magnetic flux or position and current is the best feedback configuration for controlling the EVA. A comparison of current and magnetic flux is then presented in Sec. IV, showing that magnetic flux is better than current for feedback. Sec. V then presents a controller to demonstrate how to best combine the use of position and magnetic flux.

II. EVA Model

Using the model developed by Wang [16], the dynamics of the EVA are described by

$$\frac{dz}{dt} = v$$

$$\frac{di}{dt} = \frac{V - ri + \chi_1(i,z)\,v}{\chi_2(i,z)} \tag{1}$$

$$\frac{dv}{dt} = \frac{1}{m}\left(-F_{mag}(i,z) + k_s(l-z) - bv\right) \tag{2}$$

where z (m) is the distance between the armature and the lower coil, v (m/s) is the velocity of the armature, i (A) is the current in the lower coil, m (kg) is the combined mass of the armature and valve, F_{mag} (N) is the magnetic force generated by the lower coil, k_s (N/m) is the spring constant, l (m) is half the total armature travel, b (kg/s) is the damping coefficient, V (V) is the voltage applied to the lower coil, r (Ω) is the combined resistance of the wiring and magnetic coil, $\chi_1 v$ (V) is the back-EMF effect due to the armature motion, and χ_2 (H) is the inductance of the magnetic coil. Numerical values for all constants can be found in Table I. Without loss of generality, this model neglects the dynamics of the upper coil as only one electromagnet is used to stabilize the armature at any given

time. The back-EMF, inductance, and magnetic force are given by

$$\chi_1(i,z) = \frac{2k_a i}{(k_b+z)^2} \quad \chi_2(z) = \frac{2k_a}{k_b+z} \tag{3}$$

$$F_{mag}(i,z) = \frac{k_a i^2}{(k_b+z)^2} \tag{4}$$

where k_a and k_b are constants fit based on experimental data [16].

To contrast the use of current and flux in the control, the dynamics of the EVA expressed in terms of magnetic flux are

$$\frac{dz}{dt} = v$$

$$\frac{d\lambda}{dt} = V - \frac{\lambda(k_b+z)r}{2k_a} \tag{5}$$

$$\frac{dv}{dt} = \frac{1}{m}\left(-F_{mag}(\lambda) + k_s(4-z) - bv\right) \tag{6}$$

where

$$F_{mag}(\lambda) = \frac{\lambda^2}{4k_a} \tag{7}$$

and λ (V-sec) is the magnetic flux. Converting from flux to current is facilitated by the relationship [16]

$$\lambda = \frac{2k_a i}{k_b+z}. \tag{8}$$

TABLE I

NUMERICAL VALUES FOR CONSTANTS USED IN THE MODEL.

Parameter	Numerical value	Parameter	Numerical value
m	0.27 kg	k_a	$14.96 \cdot 10^{-6}$ Nm^2/A^2
k_s	$158 \cdot 10^3$ N/m	k_b	$4.0 \cdot 10^{-5}$ m
l	$4.0 \cdot 10^{-3}$ m	r	6.0 Ω
b	7.53 kg/s		

Defining

$$x_\lambda = \begin{bmatrix} z - z_{eq} & \lambda_l - \lambda_{eq} & v \end{bmatrix}^T$$

$$x_i = \begin{bmatrix} z - z_{eq} & i_l - i_{eq} & v \end{bmatrix}^T$$

$$u = V_l - V_{eq}$$

where z_{eq}, λ_{eq}, i_{eq}, and V_{eq} are the equilibrium position, flux, current, and voltage respectively; the linear flux and current based models are given as

$$\frac{dx_\lambda}{dt} = A_\lambda x_\lambda + B_\lambda u \text{ and } \frac{dx_i}{dt} = A_i x_i + B_i u$$

where

$$A_\lambda = \begin{bmatrix} 0 & 0 & 1 \\ -\frac{r\lambda_{eq}}{2k_a} & -\frac{r(k_b+z_{eq})}{2k_a} & 0 \\ -\frac{k_s}{m} & -\frac{\lambda_{eq}}{2k_a m} & -\frac{b}{m} \end{bmatrix}$$

$$B_\lambda = \begin{bmatrix} 0 & 1 & 0 \end{bmatrix}^T$$

$$A_i = \begin{bmatrix} 0 & 0 & 1 \\ 0 & -\frac{r(k_b+z_{eq})}{2k_a} & \frac{i_{eq}}{k_b+z_{eq}} \\ -\frac{k_s}{m} + \frac{2k_a i_{eq}^2}{m(k_b+z_{eq})^3} & -\frac{2k_a i_{eq}}{m(k_b+z_{eq})^2} & -\frac{b}{m} \end{bmatrix}$$

$$B_i = \begin{bmatrix} 0 & \frac{k_b+z_{eq}}{2k_a} & 0 \end{bmatrix}^T$$

Noting that

$$\frac{\lambda_{eq}^2}{4k_a} = \frac{k_a i_{eq}^2}{(k_b+z_{eq})^2} = k_s(l - z_{eq})$$

the transfer functions from voltage to position, current, and flux are

$$P_z(s) = \frac{-1}{m} \frac{\sqrt{\frac{k_s}{k_a}(l-z_{eq})}}{s^3 + \alpha_2 s^2 + \alpha_1 s + \alpha_0} \tag{9}$$

$$P_i(s) = \frac{k_b + z_{eq}}{2k_a} \frac{s^2 + \frac{b}{m}s + \frac{k_s}{m}\left(1 - \frac{2(l-z_{eq})}{(k_b+z_{eq})}\right)}{s^3 + \alpha_2 s^2 + \alpha_1 s + \alpha_0} \tag{10}$$

$$P_\lambda(s) = \frac{s^2 + \frac{b}{m}s + \frac{k_s}{m}}{s^3 + \alpha_2 s^2 + \alpha_1 s + \alpha_0} \tag{11}$$

where

$$\alpha_2 = \frac{b}{m} + \frac{r(k_b+z_{eq})}{2k_a} \quad \alpha_1 = \frac{br(k_b+z_{eq})}{2k_a m} + \frac{k_s}{m}$$

$$\alpha_0 = \frac{k_s r(k_b + 3z_{eq} - 2l)}{2k_a m}. \tag{12}$$

Based on the sign of the coefficient α_0, Eqn. (12), the system is unstable for

$$z_{eq} < \frac{2l - k_b}{3}$$

Since $k_b \ll l$[1], the system is unstable for all equilibrium positions less than 1/3 the total armature travel away from either electromagnet.

III. DESIGN SPECIFICATIONS

From Sec. I, closed-loop control of the EVA is necessary to eliminate large impacts between the armature and magnetic coils. Additionally, the transition time from open/closed to closed/open must remain small to allow for operation at high engine speeds [15]. Explicitly, these specifications are given as:

1) The impact velocity between the armature and magnet coil must be comparable to the impact velocity achieved in a conventional cam driven valve train at idle, approximately 0.1 m/s.
2) The valve transition time from open/closed to closed/open must be approximately 4 ms.

In terms of more conventional control specifications:

1) The closed-loop step response should have no overshoot.
2) The dominant closed-loop poles should have a natural frequency of at least 785 rad/s.

The transition time from open/closed to closed/open is primarily determined by the natural response of the mechanical components of the system. The natural frequency of the mass, spring, damper subsystem has been intentionally chosen to complete the transition in approximately 4 ms. This avoids using the magnetic coils to increase the response time

[1]See Appendix.

thereby minimizing the power consumption. The unforced natural frequency of the mechanical subsystem is

$$w_n = \sqrt{k_s/m} = 766 \text{ rad/s}.$$

This implies that the free response of the armature will oscillate between the two magnetic coils with a period of 8.2 ms, or that the transition time from one side to the other is 4.1 ms. Rather than 4.1 ms, the dominant closed-loop poles should have a natural frequency of at least 785 rad/s to complete the transition in 4 ms.

Typically in EM applications, the dynamics of the electrical subsystem are significantly faster than the dynamics of the mechanical subsystem and are assumed to be negligible [3], [8], [13], [14]. Plotting the frequency response of the transfer functions given in Eqns. (9), (10), and (11), see Fig. 2, no such bandwidth separation exists and the electrical dynamics are not negligible. In Fig. 2, each transfer function has been normalized by its respective dc-gain. The lack of bandwidth separation occurs due to the stiff springs and the large inductance of the magnetic coils. To allow for operation at high engine speeds, the EVA uses extremely stiff springs thereby increasing the response time of the mechanical subsystem. In contrast, the magnetic coils act as large inductors thereby slowing the response time of the electrical subsystem.

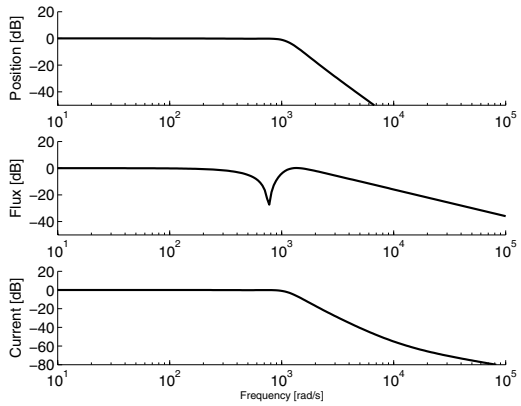

Fig. 2. Open-loop frequency response from voltage to position, flux, and current for $z_{eq} = 0$.

Consider the problem of controlling the approach of the armature as it comes into contact with the electromagnet. Using a position measurement alone would require significant control effort because the relative degree of the transfer function from voltage to position is equal to three. To extend the bandwidth of the system past the frequency at which the position gain starts to decrease without incurring excessively large control signals, it is thus desirable to use an additional flux or current measurement. The transfer functions from voltage to these measurements have relative degree one. However, it is not obvious whether or not flux or current is the better choice as the transfer function from voltage to flux exhibits an anti-resonance and the transfer function from voltage to current initially rolls off at 60 db/decade.

IV. Current vs. Magnetic Flux

This section presents a comparison of current and magnetic flux. Magnetic flux is shown to be better for feedback based on bandwidth considerations, non-minimum phase zeros, and errors introduced via linearization.

A. Bandwidth

As previously shown in Sec. III, the high frequency roll off of each transfer function is quite different. To demonstrate this more thoroughly, the frequency response of P_z, P_λ, and P_i are shown in Fig. 3 for various equilibrium positions. Again, each transfer function has been normalized by its respective dc-gain at $z_{eq} = 0$ mm.

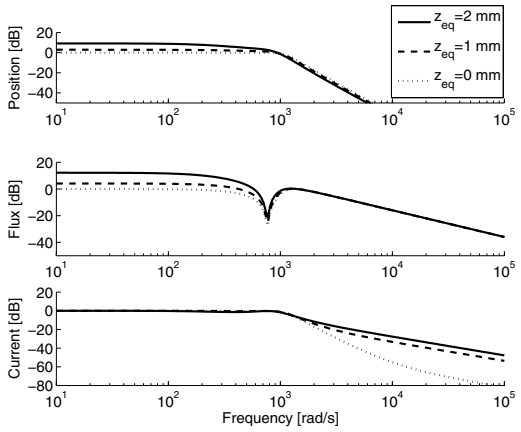

Fig. 3. Open-loop frequency response from voltage to position, flux, and current for different equilibrium positions.

As expected, the transfer function from voltage to position rolls off at 60 db/decade due to a relative degree of three. Surprisingly, the initial roll-off of P_i approaches 60 db/decade as $z_{eq} \to 0$. From inspection of the numerator of Eqn. (10), the zeros of P_i shift to high frequencies as $z_{eq} \to 0$ due to the fact that $k_b \ll l$. This in turn causes P_i to initially roll off faster than expected for a system with a relative degree of one. In contrast, the high frequency response of flux remains constant and thus will permit higher bandwidth control without incurring large high frequency control signals. Concerns about the lightly damped zeros of P_λ are addressed in Sec. V.

B. Zero Dynamics

The transfer function from voltage to current, Eqn. (10), becomes non-minimum phase (NMP) if

$$1 < \frac{2\,(l - z_{eq})}{(k_b + z_{eq})} \;\Rightarrow z_{eq} < \frac{2l - k_b}{3}.$$

Furthermore, the location of the NMP zero is dependent on the equilibrium position. For implementation, it is desirable

that a single linear controller be applied to all operating points to minimize gain scheduling. For example, one might hope that a controller designed to stabilize the plant at $z_{eq} = 0$, where the unstable pole is largest, would also stabilize the plant for larger values of z_{eq}, where the unstable pole is located closer to the jw axis. However, the controller designed for $z_{eq} = 0$ would require a relatively higher bandwidth compared to other equilibrium positions as the unstable pole takes on its largest value at $z_{eq} = 0$. If the high bandwidth controller were applied for larger values of z_{eq}, the NMP zero may lie within the system bandwidth since the NMP zero shifts to lower frequencies as $z_{eq} \to \frac{2l - k_b}{3}$. The resulting system, even if it remained stable, would have very poor sensitivity and robustness properties. In contrast, the transfer function from voltage to flux, Eqn. (11), is always minimum phase and the locations of the zeros are independent of z_{eq}.

C. Linearization Error and Singularities

In addition to differences in the frequency response, large modeling errors are introduced by linearizing the nonlinear current based model due to the factors of $k_b + z$ which appear in Eqns. (3) (4). These factors give rise to power series expressions that limit the range over which the linear model is accurate. For example, performing a Taylor series expansion of the magnetic force, Eqn. (4), about the equilibrium position results in

$$\frac{k_a i^2}{(k_b + z)^2} = \frac{k_a i_{eq}^2}{(k_b + z_{eq})^2} + k_a i_{eq}^2 \sum_{n=1}^{\infty} \frac{(-1)^n (n+1) \Delta z^n}{(k_b + z_{eq})^{n+2}}$$

where $\Delta z = z - z_{eq}$. Using the methodology of [12], the power series is convergent iff

$$0 < z < k_b + 2z_{eq}.$$

Outside of this range, the power series is divergent. Although not shown, several additional power series appear in the full Taylor series expansion used to linearize the nonlinear model, many of which are convergent over the same range. In the case of $z_{eq} = 0$ the linearization is only accurate for $0 < z < k_b$, where from Table I, $k_b = 0.04$ mm. In contrast, the only nonlinear terms that appear in the flux based model are a λ^2 term in Eqn. (7) and a bilinear term λz in Eqn. (5), both of which have a finite Taylor series expansion.

To avoid introducing this error, nonlinear control based on current could be used. However, problems again arise due to the term $k_b + z$. To better understand let us introduce the scaled parameters

$$\begin{array}{ll} \hat{z} = z \cdot 10^3 & \hat{k_s} = k_s \cdot 10^{-3} \\ \hat{l} = l \cdot 10^3 & \hat{k_b} = k_b \cdot 10^3 \\ \hat{k_a} = k_a \cdot 10^6 & \end{array}$$

and substitute Eqns. (3) (4) into Eqns. (1) (2) resulting in

$$\frac{dv}{dt} = \frac{1}{m} \left(-\frac{\hat{k_a} i^2}{\left(\hat{k_b} + \hat{z}\right)^2} + \hat{k_s} \left(\hat{l} - \hat{z}\right) - bv \right) \tag{13}$$

$$\frac{di}{dt} = \left(\frac{(V - ri)\left(\hat{k_b} + \hat{z}\right)}{2\hat{k_a}} + \frac{iv}{\hat{k_b} + \hat{z}} \right) \cdot 10^3. \tag{14}$$

The position is now measured in mm, which is more appropriate as position ranges between 0 to 8 mm, velocity between -5 to 5 m/s, and current between 0 to 15 Amps. Let us replace the term $\hat{k_b} + \hat{z}$ with the small parameter $\varepsilon = \hat{k_b} + \hat{z}$, as $\hat{k_b} \ll 1$ and $\hat{z}$ is approaching zero, resulting in

$$\frac{dv}{dt} = \frac{1}{m} \left(-\frac{\hat{k_a} i^2}{\varepsilon^2} + \hat{k_s} \left(\hat{l} - \hat{z}\right) - bv \right) \tag{15}$$

$$\frac{di}{dt} = \left(\frac{(V - r)\,\varepsilon}{2\hat{k_a}} + \frac{iv}{\varepsilon} \right) \cdot 10^3. \tag{16}$$

Physically, as the armature approaches the electromagnet (ε goes to zero) the back-EMF effect dominates the response of the current dynamics. The velocity has a disproportionately larger effect (division by ε) than the command voltage (multiplication by ε), making it difficult to control the current near the electromagnet. This is counterbalanced by the fact that the magnetic force is inversely proportional to ε^2, making large changes in the current unnecessary. Although these effects may cancel each other, they may be difficult to balance when designing a controller. Furthermore, this agrees with the analysis of Sec. IV-A showing that the transfer function from voltage to current loses some of its high frequency content as $z_{eq} \to 0$.

In contrast, the term $\hat{k_b} + \hat{z}$ appears only once in the magnetic flux based representation. Replacing it with the vanishing parameter ε in Eqns. (5) (6) results in

$$\frac{dv}{dt} = \frac{1}{m} \left(-\frac{\hat{\lambda}^2}{4\hat{k_a}} + \hat{k_s} \left(\hat{l} - \hat{z}\right) - bv \right) \tag{17}$$

$$\frac{d\lambda}{dt} = \left(V - \frac{\hat{\lambda} r \varepsilon}{2\hat{k_a}} \right) \cdot 10^3 \tag{18}$$

where $\hat{\lambda} = \lambda \cdot 10^3$. Here the competing effects of the changing current dynamics have been balanced and the influence of the command voltage and magnetic force remain constant as $\hat{z} \to 0$. Again, this agrees with the analysis of Sec. IV-A showing that the high frequency response of flux remains constant as $z_{eq} \to 0$.

V. Position and Flux Based Feedback

From the analysis of Sec. IV, the feedback configuration of position and flux is more advantageous than that of position and current. To illustrate how to best combine the use of position and flux, an example control structure is presented in this section.

In feeding back position and flux, we wish to avoid large control signals that may result from inverting the lightly

damped zeros of P_λ and/or the 60 db/decade roll-off of P_z. Using classical control techniques, it may be possible to avoid canceling the lightly damped zeros and/or inverting the 60 db/decade roll-off, but it isn't obvious how to proceed since there is no clear bandwidth separation between the two loops. However, modern control techniques tend to cancel the open-loop zeros which would introduce lightly damped poles into the controller. To avoid this, a state feedback/reduced order observer based compensator is used. Measuring position and flux, the reduced order observer is used to estimate only the armature velocity. Hence, the reduced order observer is first order and can not introduce lightly damped poles.

Following the methodology for designing reduced order observers in [1], a state feedback is selected to place the closed-loop poles at -784, -786, and -4000 rad/s. The dominant poles are then slightly over damped and have the appropriate natural frequency. In selecting the output injection gain matrix, there is an extra degree of freedom as the observer has only one state but both position and flux can be used to drive the estimation error to zero. Rather than setting one element of the output injection matrix to zero, a Kalman filter is used to select the output injection matrix assuming that the covariances of the process noise and measurement noise are equal to the identity matrix. This places the closed-loop pole associated with the observer at -1000 rad/s.

The state feedback/reduced order observer based compensator can then be broken into two components as illustrated in Fig. 4. The input voltage, u, is thus given by

$$u = C_z(s)\, z + C_\lambda(s)\, \lambda.$$

To better understand how the controller utilizes each feedback loop, the loop gains of position and flux, given by

$$L_z = C_z P_z$$
$$L_\lambda = C_\lambda P_\lambda,$$

are shown in Fig. 5. In addition, Fig. 5 includes the summation of the two loops to demonstrate how the controller combines the two feedback signals. As expected, the controller utilizes position near the anti-resonance to avoid inverting the lightly damped zeros of P_λ, while utilizing flux to avoid inverting the 60 db/decade high frequency roll-off of P_z. Hence the controller is able to achieve a much more reasonable loop gain by using both position and flux.

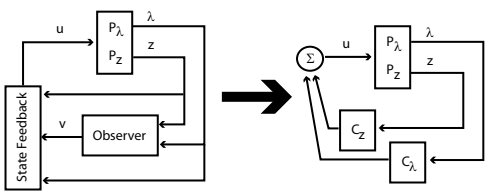

Fig. 4. Position and flux feedback structure.

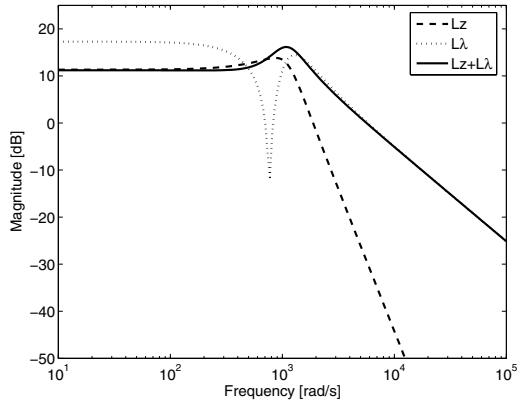

Fig. 5. Loop gains of the position and flux feedback paths.

Fig. 6 compares the frequency response of L_z and L_λ to P_z and P_λ. Although the controller does increase the dc-gain significantly, it does not alter the lightly damped zeros of P_λ or the roll-off of P_z.

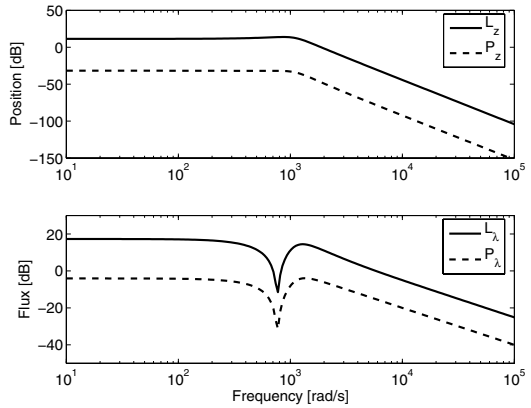

Fig. 6. Loop gain of the position and flux feedback paths versus open-loop dynamics.

VI. Measuring Magnetic Flux

As measuring current is typically less expensive than measuring flux, the following methodology for reconstructing flux is suggested. Using Eqns. (4) and (7) the magnetic flux can be reconstructed as

$$\lambda = 2\sqrt{k_a F_{mag}(i, z)}. \tag{19}$$

This relationship is used instead of Eqn. (8) as the mapping $F_{mag}(i, z)$ can include higher order effects such as magnetic saturation using look-up tables and piece-wise continuous functions [16].

VII. Conclusion

Based on the analysis of various potential feedback signals, a combination of position and magnetic flux was

shown to be the best feedback configuration. The use of the combination of position and current was shown to be less advantageous due to bandwidth considerations, NMP dynamics, and large modeling errors introduced by linearizing the system. In addition, an example control structure was proposed to demonstrate how to best combine the use of position and magnetic flux.

VIII. Appendix

Several of the issues raised in this paper depend on the fact that $k_b \ll 1$. The pertinent question is therefore whether this is a flaw of the actuator design or if it is inherent to the system. To answer this question, let us explore the relationship given in Eqn. (8) in more detail.

From [16], current and magnetic flux are related by

$$i = \frac{\lambda}{N_{coil}^2}\left(\Re_{core} + \Re_{arm} + \Re_{gap}\right)$$

based on the magnetic circuit shown in Fig. 7, where N_{coil} is the number of turns in the magnetic coil, $\Re_{core}$ is the reluctance of the core, $\Re_{arm}$ is the reluctance of the armature, and $\Re_{gap}$ is the reluctance of the gap. Neglecting the effects of magnetic saturation, $\Re_{core}$ and $\Re_{arm}$ are approximately constant and $\Re_{gap}$ is proportional to the distance between the armature and magnetic coil. Written explicitly

$$\Re_{core} = \frac{l_{core}}{\mu_{core} S_{core}},\ \Re_{arm} = \frac{l_{arm}}{\mu_{arm} S_{arm}},\ \Re_{gap} = \frac{2z}{\mu_o S_{gap}}$$

where l_{core} (m) is the mean length of the circuit loop through the magnetic core, l_{arm} (m) is the mean length of the circuit loop through the armature, μ_{core} (H/m) is the permeability of the magnetic core, μ_{arm} (H/m) is the permeability of the armature, μ_o (H/m) is the permeability of free space, S_{core} $\left(\mathrm{m}^2\right)$ is the cross-sectional area of the flux path through the magnetic core, S_{arm} $\left(\mathrm{m}^2\right)$ is the cross-sectional area of the flux path through the armature, and S_{gap} $\left(\mathrm{m}^2\right)$ is the cross-sectional area of the flux path through the gap. Therefore the constants k_a and k_b are defined as

$$k_a = \frac{1}{4}\mu_o S_{gap} N_{coil}^2 \tag{20}$$

$$k_b = \frac{\mu_o S_{gap}}{2}\left(\frac{l_{core}}{S_{core}\mu_{core}} + \frac{l_{arm}}{S_{arm}\mu_{arm}}\right). \tag{21}$$

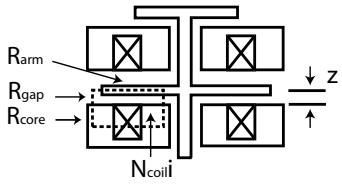

Fig. 7. Magnetic Circuit of the EVA.

Since the armature and core are presumably manufactured from a similar ferro-magnetic material, it is assume that

$$\mu_{core} \approx \mu_{arm} \approx \mu_o \mu_r$$

where μ_r is the relative permeability of the material. Therefore Eqn. (21) reduces to

$$k_b = \frac{S_{gap}}{2}\left(\frac{l_{core}}{S_{core}\mu_r} + \frac{l_{arm}}{S_{arm}\mu_r}\right).$$

Since S_{gap}, S_{core}, and S_{arm} are approximately equal and l_{arm} and l_{core} are also approximately equal,

$$O\left(k_b\right) = O\left(\mu_r^{-1}\right)$$

where $O\left(\cdot\right)$ is the order of magnitude operator. Therefore we expect $k_b \ll 1\,\mathrm{mm}$ regardless of the actuator design since the relative permeability of materials used in EM actuators are typically on the order of 10^3 [17].

References

[1] J. Bay, *Fundamentals of linear state space systems*, 1st ed. McGraw-Hill, 1999.

[2] S. Butzmann, J. Melbert, and A. Kock, "Sensor-less control of electromagnetic actuators for variable valve train," *SAE 2000-01-1225*.

[3] S. Green and K. Craig, "Robust, digital nonlinear control of magnetic-levitation systems," *ASME Journal of Dynamic Systems, Measurement and Control*, vol. 120, no. 4, pp. 488–495, Dec. 1998.

[4] W. Hoffmann, K. Peterson, and A. Stefanopoulou, "Iterative learning control for soft landing of electromechanical valve actuator in camless engines," *IEEE Transactions on Control Systems Technology*, vol. 11, no. 2, pp. 174–184, March 2003.

[5] M. Levin and M. Schechter, "Camless engine," *SAE 960581*, 1996.

[6] L. Mianzo, "A unifi ed hamiltonian framework for h2 and h-infi nity preview control algorithms with application to a variable valve timing engine," Ph.D. dissertation, University of Michigan, 2002.

[7] M. Montanari, F. Ronchi, C. Rossi, and A. Tonielli, "Control of a camless engine electromechanical actuator: Position reconstruction and dynamic performance analysis," *IEEE Transactions on Industrial Electronics*, vol. 51, no. 2, pp. 299–311, April 2004.

[8] K. Nakashima, T. Tsujino, and T. Fujii, "Multivariable control of a magnetic levitation system using closed loop identifi cation and hinf control theory," *Conference on Decision and Control*, pp. 3668–3673, December 1996.

[9] K. Peterson and A. Stefanopoulou, "Rendering the electromechanical valve actuator globally asymptotically stable," *Proc. IEEE Conference on Decision and Control*, pp. 1753–1758, Dec. 2003.

[10] ——, "Extremum seeking control for soft landing of an electromechanical valve actuator," *Automatica*, To appear as a brief paper in 2004.

[11] K. Peterson, A. Stefanopoulou, Y. Wang, and T. Megli, "Output observer based feedback for soft landing of electromechanical camless valvetrain actuator," *Proceedings of 2002 ACC*, pp. 1413–1418, May 2002.

[12] Ross, *Elementary analysis: the theory of calculus*. Springer, 2000.

[13] C. Tai and T. Tsao, "Control of an electromechanical camless valve actuator," *Proceedings American Control Conference*, May 2002.

[14] M. Velasco-Villa, R. Castro-Linares, and L. Corona-Ramirez, "Modeling and passivity based control of a magnetic levitation system," *IEEE Conference on Control Applications*, pp. 64–69, 2001.

[15] Y. Wang, T. Megli, M. Haghgooie, K. Peterson, and A. Stefanopoulou, "Modeling and control of electromechanical valve actuator," *SAE 2002 Transactions - Journal of Engines, SAE 2002-01-1106*, 2002.

[16] Y. Wang, A. Stefanopoulou, M. Haghgooie, I. Kolmanovsky, and M. Hammoud, "Modeling of an electromechanical valve actuator for a camless engine," *Int'l Symposium on Advanced Vehicle Control*, no. 2, Aug 2000.

[17] R. Wolfson and J. Pasachoff, *Physics for Scientists and Engineers*, 2nd ed. Harper Collins, 1995.